Walkoff-Compensated Dispersion-Mapped Quadratic Solitons

Lluis Torner, *Member, IEEE*

***Abstract*—Formation of temporal guiding-center walking solitons in tandem structures made of quadratic nonlinear crystals is investigated. The specific new effects and possibilities arising by engineering the multifrequency periodical variation of the group-velocity, group-velocity dispersion and nonlinearity existing in the tandem structures are introduced.**

***Index Terms*— Dispersion-management, quadratic solitons, quasi-group-velocity-matching, solitons, walkoff-compensation.**

THE RECENT observation by Di Trapani *et al.* [1] and by Liu *et al.* [2] of pulse self-narrowing consistent with temporal soliton formation in a quadratic nonlinear crystal under conditions for second-harmonic generation (SHG) opens a fascinating new avenue for exploration of potential applications of optical solitons mediated by quadratic nonlinearities. The experiment performed by Di Trapani *et al.* [1] was actually made in β-BaB_2O_4 pumped with 200-fs pulses at 527 nm, under conditions where both quadratic and cubic nonlinearities were claimed to contribute, while Liu *et al.* [2] used $LiIO_3$ pumped with 100-fs pulseds at 795 nm focused to a beam waist of 40 μm to observe spatiotemporal trapping of light. Those experiments came after the observation of spatial quadratic solitons in several materials and settings during the last few years. Mathematically, spatial and temporal quadratic solitons are described by similar equations, but their experimental formation faces different challenges.

The main difficulties encountered to form temporal quadratic solitons are the small group-velocity-dispersion (GVD) exhibited by the known materials with large quadratic nonlinearities and low absorption at optical wavelengths, together with the large group-velocity-mismatch (GVM) experienced by the multiple-frequency waves that are to mutually trap to form the solitons. The authors of [1] and [2] used achromatic phase-matching (APM), or tilted-pulse, techniques [3] to minimize the intrinsic material GVM at the operating wavelengths, while at the same time enhancing the effective GVD experienced by the two-color signals. In this letter, I discuss the formation of temporal guiding-center quadratic solitons in walkoff compensating tandem structures, in a scheme originally proposed for GVM compensation in Stankov's frequency-doubling mode-locker [4]. Feasibility of such a GVM compensation technique, which might be referred to as quasi-group-velocity-matching (QGVM), was demonstrated experimentally in CW Nd:YLF and Nd:YAG lasers with intracavity SHG in LiB_3O_5 pumped at 1050 nm [5], and in SHG with 250-fs pump pulses at 800 nm in β-BaB_2O_4 [6]. In the case of soliton signals, the guiding-center scheme might find applications to light bullet formation in bulk settings with large enough GVD, including multiple-pass geometries, where to the best of my knowledge APM techniques with focused beams are yet to be developed. Another novel possibility is to use a combination of QGVM and APM in geometries where the latter are to maximize the GVD, and thus, leave a moderate GVM. Last but not least, walkoff compensated quadratic solitons experience a periodically varying GVD, opening the important new possibility of soliton shaping and control by engineering the GVD map.

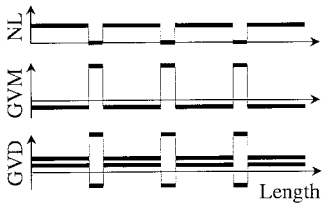

Fig. 1. Sketch of the nonlinearity, group-velocity-mismatch, and GVD maps encountered by the walkoff compensated solitons.

GVM compensation in tandem structures is based on the periodic reversal of the pulse walkoff. Contrary to its spatial analog where pure sign reversal of the Poynting vector walkoff can be achieved by proper crystal rotation, in general QGVM requires alternate compensating domains of different lengths, which can be made with different materials, or with the same material but with different crystal orientations. In either case, not only the GVM varies periodically along the tandem structure, but also the GVD, the phase-mismatch, and the nonlinearity do. In practice, an ideal setup might be composed of alternating domains of two types: the first type optimized for high quadratic nonlinearity, the second type optimized for GVM compensation and GVD engineering. In such a case, the strength of the parametric mixing is drastically suppressed in the compensating pieces, which thus can be considered as being linear. Such a GVM-GVD-NL map is illustrated in Fig. 1.

Here, I restrict myself to one-dimensional geometries, which correspond to pulsed propagation in channel waveguides or in bulk media with wide beams, and to type I SHG. The evolution

Manuscript received May 4, 1999. This work was supported by the Government of Spain under Contract PB95-0768.

The author is with the Laboratory of Photonics, Department of Signal Theory and Communications, Universitat Politecnica de Catalunya, Gran Capitan UPC-D3, Barcelona, ES 08034, Spain.

Publisher Item Identifier S 1041-1135(99)07750-2.

of the slowly varying light signals can be described by

$$i\frac{\partial a_1}{\partial \xi}+\frac{\alpha_1(\xi)}{2}\frac{\partial^2 a_1}{\partial s^2}-i\delta_1(\xi)\frac{\partial a_1}{\partial s}+d_1(\xi)a_1^* a_2\exp(-i\beta\xi)=0, \quad (1)$$

$$i\frac{\partial a_2}{\partial \xi}+\frac{\alpha_2(\xi)}{2}\frac{\partial^2 a_2}{\partial s^2}-i\delta_2(\xi)\frac{\partial a_2}{\partial s}+d_2(\xi)a_1^2\exp(i\beta\xi)=0 \quad (2)$$

where a_1 and a_2 are the normalized envelopes of the fundamental frequency (FF) and second-harmonic (SH) waves, respectively. The parameters δ_ν and α_ν, $\nu=1,2$, are related to the GV and GVD existing at both frequencies, d_ν are scaled nonlinear coefficients, and β is the normalized phase mismatch between the waves. The scaled coordinates are $s=t/\tau$, where τ is a pulsewidth, and $\xi=z/l_{d1}$, with $l_{d1}=\tau^2/|k_1''|$, where $k_1''=\partial^2 k_1/\partial\omega$, is the dispersion length at the FF. The system (1)–(2) conserves the total energy $I_a=\int(|a_1|^2+|a_2|^2)\,ds$.

To implement a QGVM scheme consider an optically contacted [7], tandem structure with alternating domains of lengths $l_<$ and $l_>$. The length of each domain is dictated by the GVM parameter $\Delta v=1/v_{g,2}-1/v_{g,1}$, $v_{g,\nu}$ being the corresponding group velocity. One needs $l\sim\tau/\Delta v$ for efficient walkoff compensation and $l_<\gg l_>$ to minimize the overall nonlinearity reduction. For example, in the case of QGVM in LiB_3O_5 studied by Cerullo *et al.* [5], where $\Delta v\sim 55$ fs/mm, both passive β-BaB_2O_4 and calcite, having $\Delta v\sim -280$ fs/mm and $\Delta v\sim -450$ fs/mm, respectively, were identified as potential compensating crystals. The above values yield $\Delta v_>/\Delta v_<\sim 5$ for β-BaB_2O_4, and higher ratios for calcite. The geometry used by Gehr *et al.* [6] in active–passive β-BaB_2O_4 yields $\Delta v_>/\Delta v_<\sim 0.5$, thus the overall nonlinearity is importantly reduced when $l_>\approx 2l_<$, but it allows simultaneous GVM and Poynting vector walkoff compensation. In the numerics below I set $\Delta v_>/\Delta v_<=10$.

For moderate GVD-GVM-NL maps the average pulse evolution in the tandem structure is given by governing equations formally identical to (1)–(2) but with the fast-varying fields a_ν and periodically varying parameters α_ν, δ_ν, d_ν, substituted by the guiding-center fields $a_\nu^{(0)}$ and the averaged values of the parameters $\alpha_\nu^{(0)}$, $\delta_\nu^{(0)}$, $d_\nu^{(0)}$ over the map [8]. We assume optimized GVM compensation hence set $\delta_\nu^{(0)}=0$. We also assume that Kleimann symmetry holds, thus $d_2=d_1$. The explicit dependences on the averaged GVD at the FF, and on the averaged nonlinearity can be readily eliminated from the averaged evolution equations by rescaling the propagation coordinate and fields. Let $\zeta=\alpha_1^{(0)}\xi$, and $q_\nu=d_\nu^{(0)}a_\nu^{(0)}/\alpha_1^{(0)}$. The resulting evolution equations are those that hold in a uniform medium with $\alpha_1=1$, and with the phase-mismatch $\tilde\beta=\beta/\alpha_1^{(0)}$ and the GVD at the SH frequency $\tilde\alpha_2=\alpha_2^{(0)}/\alpha_1^{(0)}$. The corresponding guiding-center stationary soliton solutions are thus identical to those existing in uniform structures, but with the above GVD and phase-mismatch parameters, plus the energy shift $I_a=[\alpha_1^{(0)}(1+\Delta l)]^2 I_q$, where $\Delta l=l_>/l_<$. Such energy shift stands for the overall GVD experienced by the pulses and for the soliton tunneling through the walkoff compensating linear pieces. One needs short domains as those examined here for the lowest order guiding-center model to hold. Higher order corrections arising with large domains can be taken into account.

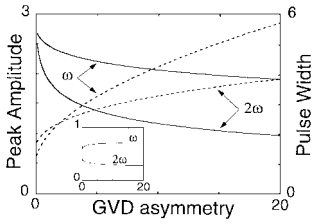

Fig. 2. Peak amplitude (solid lines) and FWHM (dashes) of the FF and SH pulses forming the stationary dispersion-mapped guiding-center solitons as a function of the GVD ratio $\tilde\alpha_2$, for a fixed phase-mismatch and soliton energy. $\beta=0$, $I_q=15$. Inset: Variation of the fraction of the total energy carried by each wave.

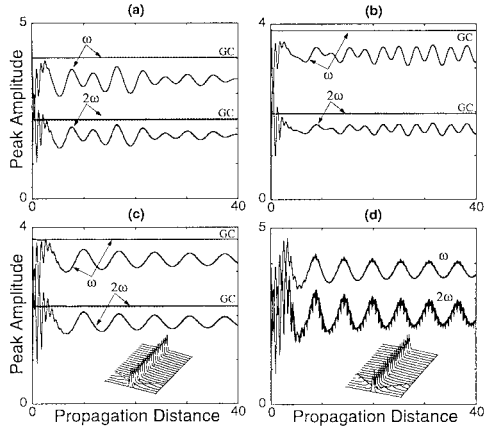

Fig. 3. Evolution of the peak amplitudes of the FF and SH pulses as a function of propagation distance, for different two-color GVD maps. Only FF input light. Curves labeled GC: evolution of the corresponding guiding-center solitons. GVD maps $[\alpha_{1<},\alpha_{2<},\alpha_{1>},\alpha_{2>}]$: (a) $[1,2,1,-10]$; (b) $[0.1,0.2,10,20]$; (c) $[-0.5,-0.5,20,10]$; (d) $[1,2,1,-22]$. Domain lengths: $\xi_<=0.1$, $\xi_>=0.01$. Through all the paper the length of the domain located at $\xi=0$ is halved. $\delta_{1,2}=0$, $\beta=3$, $I_a=30$. Insets: detailed evolution of the FF pulse.

The effect of the GVD asymmetry $\tilde\alpha_2$ on the shape of the solitons is shown in Fig. 2, which displays the behavior of the pulse peak amplitude and width as a function of $\tilde\alpha_2$. The plot reveals that when the parameter $\tilde\alpha_2$ increases for a fixed energy the soliton pulses feature smaller peak amplitudes and broader shapes. However, as shown in the inset, the pulses change shape in such a way that they keep the fraction of energy at each frequency almost constant, similar to what is found for elliptical light bullets. The plot corresponds to $\beta=0$, but similar features are obtained at other values of β. One thus arrives at the conclusion that engineered values of $\tilde\alpha_2$ allow soliton shaping with minimal energy redistribution.

The formation of solitons in a variety of compensating maps exposes the great potential of the scheme. Fig. 3 shows a few illustrative important examples. To isolate the effects due to the GVD map, we first set $\delta=0$. Light is input only at the FF with the shape $a_1(0)=A\,\mathrm{sech}(s)$ in structures with domain lengths $\xi_<=0.1$, $\xi_>=0.01$. The evolutions of the corresponding guiding-center solitons are also shown. Fig. 3(a) corresponds to a weak GVD map where the compensating pieces perturb only slightly the pulse evolution. Pulses readily tunnel the linear parts and the guiding-center soliton propagates steadily.

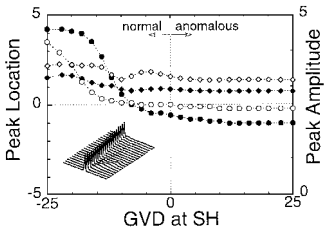

Fig. 4. Peak location (bullets) and peak amplitude (diamonds) at $\xi = 10$ of the FF pulse forming a guiding-center walking soliton excited with only FF input light, as a function of the GVD of the compensating crystals at the SH frequency. GVD map: $[1, 2, 1, \alpha_{2>}]$. GVM map: $[0, 0, 10, -100]$. Open symbols: $\xi_< = 0.1$, $\xi_> = 0.01$; filled: $\xi_< = 0.2$, $\xi_> = 0.02$. $\beta = 3$, $I_a = 30$. Inset: Detailed evolution of the FF pulse with $\alpha_{2>} = -15$, $\xi_< = 0.2$, $\xi_> = 0.02$.

Fig. 3(b)–(d) illustrates some of the new possibilities offered by engineered maps. Fig. 3(b) shows the robust formation of solitons in structures composed of weakly dispersive active crystals and of highly dispersive passive crystals, thus yielding a moderate overall GVD. Fig. 3(c) shows soliton formation in the more extreme situation encountered when the active crystals exhibit normal GVD. The important conclusion is that one might optimize the active pieces for the highest nonlinearity and the passive pieces for optimal GVM compensation and GVD engineering. Fig. 3(d) corresponds to a strong GVD map such that the overall GVD at the SH frequency is normal. Yet, soliton-like propagation under such conditions is clearly visible in the plot, opening the door of quadratic soliton formation in strong GVD maps, and with overall normal GVD.

The influence of the full GVM-GVD-NL maps on the soliton formation is illustrated in Fig. 4. The plot shows the behavior of the peak amplitude and temporal location of the FF pulse at $\xi = 10$ as a function of the GVD of the compensating pieces at the SH frequency. The SH pulse evolves locked to the FF and hence is not shown. Light is input only at the FF with constant energy $I_a = 30$ in a structure with a phase-mismatch at the active pieces of $\beta = 3$. With large domains, the efficiency of the QGVM technique decreases so that the pulses experience a correspondingly large residual walkoff that moves them away from their time slot. However, guiding-center walking solitons do form even with $\delta_<\xi_< = \delta_>\xi_> = 2$. Fig. 4 reveals that walkoff compensated soliton formation is robust against variations in the GVD maps, particularly at the anomalous side. Large negative (normal) GVD values that render the overall GVD at the SH frequency very small or even normal are shown to have a stronger influence on the pulse evolution, in particular by compressing the pulses as predicted by Fig. 2, and by increasing the existing residual walkoff. However, Fig. 4 reveals that soliton-like propagation is clearly obtained even under such conditions. The inset displays a detailed evolution in a typical example. Similar results were obtained at a variety of other values of β, I, GVM, NL, and GVD maps different than those reported here.

In conclusion, robust temporal guiding-center walking solitons are predicted to form in properly tailored QGVM tandem structures made of quadratic nonlinear crystals. Engineering the GVM, GVD and NL maps encountered by the light signals provides new strategies for quadratic soliton shaping and control. The scheme discussed might be also relevant for multiple-pass cavity and laser settings, and for multicolor light trapping in quantum systems.

ACKNOWLEDGMENT

The author acknowledges many discussions with J. Perez.

REFERENCES

[1] P. Di Trapani, D. Caironi, G. Valiulis, A. Dubietis, R. Danielius, and A. Piskarskas, "Observation of temporal solitons in second-harmonic generation with tilted pulses," *Phys. Rev. Lett.*, vol. 81, pp. 570–573, July 1998.

[2] X. Liu, L. J. Qian, and F. W. Wise, "Generation of optical spatiotemporal solitons," *Phys. Rev. Lett.*, vol. 82, pp. 4631–4634, June 1999.

[3] G. Valiulis, A. Dubietis, R. Danielius, D. Caironi, A. Visconti, and P. Di Trapani, "Temporal solitons in $\chi^{(2)}$ materials with tilted pulses," *J. Opt. Soc. Amer. B*, vol. 16, pp. 722–731, May 1999.

[4] K. A. Stankov, V. P. Tzolov, and M. G. Mirkov, "Compensation of group-velocity mismatch in the frequency-doubling modelocker," *Appl. Phys. B*, vol. 54, pp. 303–306, Apr. 1992.

[5] G. Cerullo, V. Magni, and A. Monguzzi, "Group-velocity mismatch compensation in CW lasers mode locked by second-order nonlinearities," *Opt. Lett.*, vol. 20, pp. 1785–1787, Sept. 1995.

[6] R. J. Gehr, M. W. Kimmel, and A. V. Smith, "Simultaneous spatial and temporal walk-off compensation in frequency-doubling femtosecond pulses in β-BaB_2O_4," *Opt. Lett.*, vol. 23, pp. 1298–1300, Aug. 1998.

[7] J.-J. Zondy, M. Abed, S. Khodja, C. Bonnin, B. Rainaud, H. Albrecht, and D. Lupinksky, "Walkoff-compensated type I and type II SHG using twin-crystal $AgGaSe_2$ and $KTiOPO_4$ devices," in *Proc. SPIE*, 1996, vol. 2700, pp. 66–72.

[8] A. Hasegawa and Y. Kodama, *Solitons in Optical Communications*. Oxford, U.K.: Clarendon, 1995.